

A decatungstate-type polyoxoniobate with centered manganese: $[\text{H}_2\text{Mn}^{\text{IV}}\text{Nb}_{10}\text{O}_{32}]^{8-}$ as a soluble tetramethylammonium salt

Jung-Ho Son^{*a} and William H. Casey^{*a,b}Cite this: *Dalton Trans.*, 2013, **42**, 13339

Received 3rd July 2013,

Accepted 31st July 2013

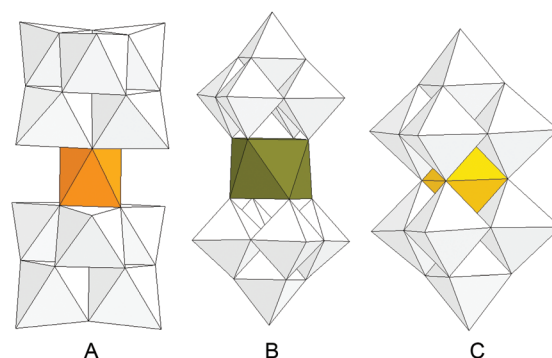
DOI: 10.1039/c3dt51798e

www.rsc.org/dalton

A highly symmetric Mn^{IV} -centered polyoxoniobate $[\text{H}_2\text{Mn}^{\text{IV}}\text{Nb}_{10}\text{O}_{32}]^{8-}$ was synthesized via hydrothermal methods as a soluble tetramethylammonium salt. The structure is similar to decatungstate structure $[\text{W}_{10}\text{O}_{32}]^{4-}$, except for the central heteroatom. The cluster is stable between $4 < \text{pH} < 10$, as was characterized with ESI-MS and UV-Vis spectroscopy.

Polyoxometalates (POMs) comprise a class of metal–oxide ions that are widely used in catalysis and material science.¹ The most familiar compounds are oxides of group 5 or 6 metals, such as vanadates, tungstates and molybdates. Unsubstituted POMs are usually diamagnetic in their most oxidized form and transition-metal-substituted POMs find use via their magnetic, electrochemical, and optical properties.²

Polyoxoniobates (PONb) are relatively less explored due to the synthetic challenge, although hexaniobate and decaniobate ions have been studied for many decades,³ in part from the pioneering work by Spinner⁴ and in spite of recent advances.⁵ Numbers of PONb substituted with main-group element have been synthesized by Nyman and coworkers.⁶ Transition-metal-substituted PONb have appeared in the literature more recently.⁷ As one of the earliest reported heteropolyoxoniobate compounds, Pope *et al.* and Stucky *et al.* reported two hexaniobate ions linked by Mn^{IV} or Ni^{IV} , *i.e.* $\text{Na}_{12}[\text{MnNb}_{12}\text{O}_{38}] \cdot 50\text{H}_2\text{O}$ (MnNb_{12} , Scheme 1A).⁸ Here, the hexaniobate ions cap and ligate the heteroatom in a sandwich-like geometry, but the heteroatom is not completely trapped in the PONb cage.⁹ This sandwich compound resembles the Weakley–Yamase type tungstate structure, $[\text{Ln}(\text{W}_5\text{O}_{18})_2]^{n-}$,



Scheme 1 Polyhedral drawing of MnNb_{12} (A), $[\text{Ln}(\text{W}_5\text{O}_{18})_2]^{7-}$ (B) and MnNb_{10} (C).

Scheme 1B) where two W_5O_{18} units are linked by a central lanthanide ion.¹⁰ Pope *et al.* synthesized a $[\text{Mn}(\text{CO})_3]^+$ -capped hexaniobate more recently.¹¹ However, complete encapsulation of manganese within the PONb framework has not yet been achieved. Echoing the goals of the Pope *et al.*,¹¹ manganese substitution in PONb might benefit attempts to sequester dangerous nuclides, such as ^{99}Tc , in nuclear waste as niobates are generally stable at basic-pH conditions.

Herein we report a new type of Mn^{IV} -substituted PONb cluster, $[\text{H}_2\text{Mn}^{\text{IV}}\text{Nb}_{10}\text{O}_{32}]^{8-}$ [MnNb_{10} , Scheme 1C], as a tetramethylammonium (TMA) salt, $\text{TMA}_8[\text{H}_2\text{Mn}^{\text{IV}}\text{Nb}_{10}\text{O}_{32}] \cdot 22\text{H}_2\text{O}$ (**1**). This cluster ion can be viewed as two MnNb_5 Lindqvist motifs condensed by bridging oxygen atoms and sharing a Mn^{IV} site. We note that the structure of this cluster is similar to decatungstate ion,¹² $[\text{W}_{10}\text{O}_{32}]^{4-}$, which is used for photocatalyst in organic reactions.¹³ Structurally similar vanadates like $[\text{MV}_{13}\text{O}_{38}]^{7-}$ ($\text{M} = \text{Mn}^{\text{IV}}, \text{Ni}^{\text{IV}}$) are known,¹⁴ with additional vanadates surrounding the center site of the cluster shown in Scheme 1C. Decatungstate is unstable in aqueous solution and the vanadate derivative is only stable at $3 < \text{pH} < 5$.

The compound **1** was synthesized by hydrothermal reaction of the mixture of hydrous niobium oxide, KMnO_4 , TMAOH at 110°C for 3 days. We note that higher reaction temperatures lead to decomposition of the cluster over increased reaction

^aDepartment of Chemistry, University of California, Davis, One Shields Ave., Davis, CA 95616, USA. E-mail: junghoson@gmail.com, whcasey@ucdavis.edu; Fax: (+1) (530) 752 8995; Tel: (+1) (530) 752 3211

^bDepartment of Geology, University of California, Davis, One Shields Ave., Davis, CA 95616, USA

†Electronic supplementary information (ESI) available: Experimental details, ESI-MS peak assignment with calculated spectrum, UV-Vis titration data of 0.02 mM, 0.2 mM and 2 mM solution of **1**, ESI-MS of 0.2 mM solution of **1** during titration and FT-IR spectrum. CCDC 943073. For ESI and crystallographic data in CIF or other electronic format see DOI: 10.1039/c3dt51798e

times. The resulting brown solution after reaction was washed with isopropanol and extracted with ethanol. Purification to get analytically pure compound of **1** was challenging due to the similar solubility of **1** and dark colored impurity. The crystals of **1** were obtained as olive-gold colored crystals in the dark-brown viscous oily product. The dark, oily product was carefully washed with minimal amounts of ethanol to isolate crystals, since the dark colored impurity was only slightly more soluble in ethanol than **1**. We note that the previously reported reaction condition to obtain MnNb_{12} sandwich complex⁸ involved lower temperature ($\sim 90^\circ\text{C}$) and shorter reaction times (less than an hour) compared to the conditions used to synthesize **1**. We suspect that the Mn^{IV} encapsulated by the niobates results from a solution driven to a thermodynamically more stable end point by longer reaction times and higher temperatures.

The structure of **1** was determined by single crystal X-ray crystallography.[†] The cluster in **1** has manganese at the center surrounded by ten oxo-niobate frameworks, possessing idealized D_{4h} symmetry [Scheme 1C, Fig. 1]. Eight TMA ions are found in the structure of **1**, suggesting the charge of the cluster as -8 . Bond valence sum (BVS) calculation (4.059) indicates the manganese oxidation state of Mn^{IV} . Two protons on the surface of the cluster are found in the electron-density map, thus the formula of the cluster can be expressed as $[\text{H}_2\text{Mn}^{\text{IV}}\text{Nb}_{10}\text{O}_{32}]^{8-}$. These protons are bound to two $\mu_2\text{-O}$ at the opposite sides of the cluster [Fig. 1]. Central site in the cluster shows regular MnO_6 octahedron, with Mn–O lengths ranging between 1.875(3) and 1.916(3) Å and nearly orthogonal O–Mn–O angles from $89.46(12)^\circ$ to $90.55(12)^\circ$. The Mn– $\mu_2\text{-O}$ –Nb angles (103° – 105°) are smaller than Nb– $\mu_2\text{-O}$ –Nb angles (113° – 120°), because of the significantly short Mn– $\mu_6\text{-O}$ (1.876(3) Å) compared to Nb– $\mu_6\text{-O}$ (2.475(3) and 2.484(3) Å) in *trans* position.

We note that the cluster MnNb_{12} has similar, but more regular, Mn–O lengths of 1.863(26), 1.865(25) and 1.878(24) Å than MnNb_{10} . However, the MnO_6 in MnNb_{12} is elongated between the two hexaniobates, with two distinct O–Mn–O angles around 83° and 96° . This elongation is explained by Flynn and Stucky as being caused by the electrostatic repulsion of two hexaniobate units, which results in the axial stretching of the MnO_6 octahedron.^{8d} The coordination to Mn^{IV} in MnNb_{12} causes distortion within the hexaniobate ions, with the three oxygen atoms of the hexaniobates coordinating to

Mn^{IV} being closer to each other, with O...O distances within 2.45–2.50 Å in the MnNb_{12} cluster, while the distances are normally 2.75–2.80 Å for uncoordinated $\mu_2\text{-O}$ in the same hexaniobate units.

MnNb_{10} cluster is structurally similar to decatungstate except the existence of central Mn^{IV} . W–O bonds in decatungstate range 1.69–2.34 Å, while Nb–O bonds in **1** are slightly longer within a large 1.75–2.48 Å range due to the less positively charged Nb^{V} compared to W^{VI} . PONb usually have higher negative charges than polyoxotungstates for the same reason. For example, a $[\text{Nb}_{10}\text{O}_{32}]$ cluster without heteroatoms reducing the charge would have high charge of -14 , compared to $[\text{W}_{10}\text{O}_{32}]^{4-}$. Thus, incorporation of the central Mn^{IV} and two surface protons lowers the overall cluster charge to -8 , thereby stabilizing it.

Electrospray-ionization mass spectrometry (ESI-MS) confirmed the identity of the cluster in the solution [Fig. 2]. The mass spectrum of **1** shows series of peaks for -4 , -3 and -2 charged ions. The series of -4 ion peaks can be explained as due to fragmentation of the relatively highly charged $\text{H}_4[\text{H}_2\text{MnNb}_{10}\text{O}_{32}]^{-4}$ ion during ionization in the ESI-MS. The mass spectrum of **1** also exhibits multiple peaks for -3 and -2 ions in higher m/z ranges, in addition to the $\text{TMA}_x\text{H}_y\text{H}_2[\text{H}_2\text{MnNb}_{10}\text{O}_{32}]^{-(8-x-y)}$ ions. These are commonly observed in the ESI-MS of the TMA salts of other PONb, but in much smaller intensities.^{7h-k} These additional multiple peaks are interpreted as CH_3^+ adduct of the cluster ions, as the peak positions and shapes match well with calculations [Fig. S1†]. Thus the $[\text{H}_2\text{MnNb}_{10}\text{O}_{32}]^{8-}$ cluster exhibits a somewhat unique behaviour in ESI-MS compared to other polyoxoniobates. Some methylated Anderson-type heteropolyoxomolybdates have been synthesized by ligand exchange with methanol.¹⁵ However, **1** exhibits the same ESI-MS spectra without contact with methanol. Thus actual existence of methylated cluster in our system is unlikely and we believe that the peaks corresponding to CH_3^+ adduct originated from the fragmentation of TMA during ionization.

The color of the aqueous solution of **1** is yellow and distinctly different from the reported orange color of MnNb_{12} ,

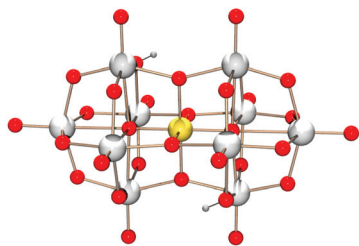


Fig. 1 Ball-and-stick model of $[\text{H}_2\text{Mn}^{\text{IV}}\text{Nb}_{10}\text{O}_{32}]^{8-}$ (yellow: Mn, large grey: Nb, red: O, small grey: H).

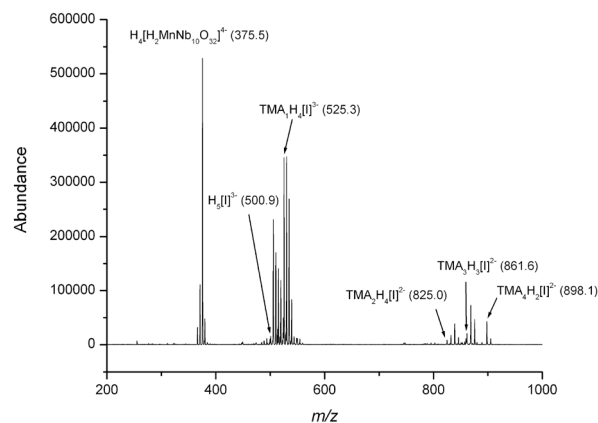


Fig. 2 ESI-MS of **1** with peak assignments. [**1**] = $[\text{H}_2\text{Mn}^{\text{IV}}\text{Nb}_{10}\text{O}_{32}]$ (0.2 mM solution of **1**, pH 7.7).



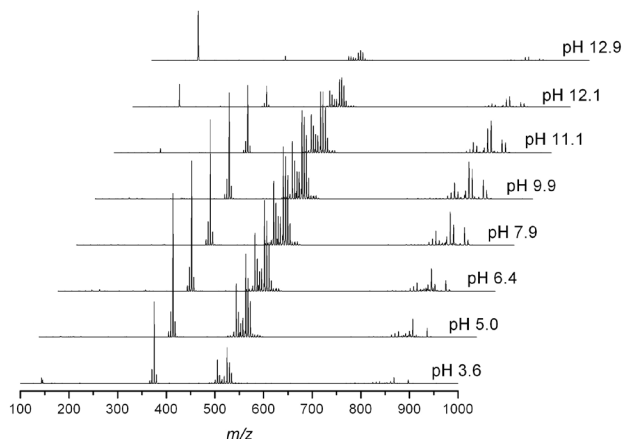


Fig. 3 ESI-MS of 2 mM solution of **1** during titration in different pH. The solution concentration change for each pH was minimized by using 1 M acid or 2.75 M base in titration. Each spectrum is an averaged signal for acquisitions of 1 min duration. The peak at 196 m/z in basic condition corresponds to TMAOH.

probably due to the slightly different Mn–O environment. UV-Vis absorption spectrum of **1** is also different from that reported for the MnNb_{12} , which has absorbances at 238, 300, 450 and 480 nm,⁸ while **1** shows absorption near 250, 300, 350 and 450 nm [Fig. S2–S4†].

The stability of the cluster was examined by using both UV-Vis and ESI-MS titration experiments. When dissolved into solution at 2 mM concentrations, the solution reaches a natural pH of 8.7. Adding acid or base to this solution leads to decomposition of the cluster, as is evident in the decreased abundance of peaks assignable to clusters in ESI-MS of 2 mM and 0.2 mM solutions [Fig. 3 and Fig. S5,† respectively]. When titrating with base, peaks assignable to the clusters significantly decrease in abundance at $\text{pH} > 11$ for a 2 mM solution of **1** and $\text{pH} > 9$ for 0.2 mM solution of **1**. ESI-MS spectra taken during an acid titration of **1** indicates that the cluster is stable until $\text{pH} \sim 5$, however, the initial golden yellow color of the solution started to fade at $\text{pH} < 7$ and changed to orange-pink color near $\text{pH} \sim 4$ during the titration of a 2 mM solution of **1** with acid, while the yellow solution color did not change with base addition until $\text{pH} \sim 13$. In addition to decomposition, we suspect that protonation of structural oxygens is affecting the color.

ESI-MS of the acidified solution indicated an increase in peaks assignable to H^+ adducts of **1**, with a decrease of the CH_3^+ -adduct peak. The increase in CH_3^+ adduct peaks during base addition is expected and attributable to the increased TMA concentration, added to the solution as a TMAOH base and then fragmented in the ionization step of ESI-MS [Fig. 3 and Fig. S5†].

Among the UV-Vis absorption bands of 0.02 mM solution of **1**, the strongest ligand-metal charge-transfer (LMCT) band at 250 nm was the most sensitive to decomposition of the cluster [Fig. S2†]. When **1** was titrated with base, the band at 250 nm decreased as pH increased, with two new bands appearing near 240 nm and 260 nm above pH 9 [Fig. S2†].

We suspect that these indicate decomposition of the cluster, in agreement with the ESI-MS results. The absorption spectra did not change significantly until acidified to pH 4.4. Below this pH, overall absorption gradually increased until the compound finally decomposed to form a colored precipitate that we assume is hydrous, manganese–niobium oxide. The behavior is similar in the higher concentration solutions, but the 2 mM solution begins to flocculate as early as pH 6.5, reflecting the higher sample concentration and existence of background salt (0.1 M TMACl), which was not used in ESI-MS titration experiment.

In summary, we report a new Mn^{IV} -substituted PONb , $[\text{H}_2\text{Mn}^{\text{IV}}\text{Nb}_{10}\text{O}_{32}]^{8-}$ as a soluble TMA salt. It has a relatively wide stability between $4 < \text{pH} < 10$ in aqueous solutions, suggesting a robust use in applications, possibly complementing the decatungstate ion.

This work was supported by an NSF CCI grant through the Center for Sustainable Materials Chemistry, number CHE-1102637.

Notes and references

†Crystal data. (1) CCDC 943073. $\text{C}_{32}\text{H}_{101}\text{N}_8\text{O}_{54}\text{MnNb}_{10}$, $M = 2446.25$, monoclinic, $a = 13.9537(6)$, $b = 34.0884(14)$, $c = 18.0134(7)$ Å, $\beta = 92.907(1)^\circ$, $U = 8557.2(6)$ Å³, $T = 88$ K, space group $P2_1/n$ (no. 14), $Z = 4$, 125 508 reflections measured, 17 489 unique ($R_{\text{int}} = 0.0391$) which were used in all calculations. The final $wR(F^2)$ was 0.0937 (all data).

- (a) M. T. Pope, *Heteropoly and Isopolyoxometalates*, Springer-Verlag, Berlin, 1983; (b) M. T. Pope and A. Müller, *Angew. Chem., Int. Ed. Engl.*, 1991, **30**, 34–48; (c) *Polyoxometalates. From Platonic Solids to Anti-Retroviral Activity*, ed. M. T. Pope and A. Müller, Kluwer Academic Publishers, Dordrecht, The Netherlands, 1994; (d) C. L. Hill, ed. Special issue on “Polyoxometalates”, *Chem. Rev.*, 1998, **98**, 1–390; (e) C. Ritchie, A. Ferguson, H. Nojiri, H. N. Miras, Y.-F. Song, D.-L. Long, E. Burkholder, M. Murrie, P. Kögerler, E. K. Brechin and L. Cronin, *Angew. Chem., Int. Ed.*, 2008, **47**, 5609–5612; (f) J.-D. Compain, P. Mialane, A. Dolbecq, I. Mbomekallé, J. Marrot, F. Sécheresse, E. Rivi  re, G. Rogez and W. Wernsdorfer, *Angew. Chem., Int. Ed.*, 2009, **121**, 3123–3127.
- (a) *Polyoxometalate Molecular Science*, ed. J. J. Borr  s-Almenar, E. Coronado, A. M  ller and M. T. Pope, Springer, 2003; (b) *Polyoxometalate Chemistry from Topology via Self-Assembly to Applications*, ed. M. T. Pope and A. M  ller, Kluwer Academic Publishers, Dordrecht, The Netherlands, 2001; (c) U. Kortz, A. M  ller, J. van Slageren, J. Schnack, N. S. Dalal and M. Dressel, *Coord. Chem. Rev.*, 2009, **253**, 2315–2327; (d) D.-L. Long, R. Tsunashima and L. Cronin, *Angew. Chem., Int. Ed.*, 2010, **49**, 1736–1758; (e) L. Cronin and A. M  ller, eds. Special issue on “Polyoxometalate cluster science”, *Chem. Soc. Rev.*, 2012, **41**(22), 7325–7648; (f) D.-L. Long and L. Cronin, eds. Special issue on “Polyoxometalates”, *Dalton Trans.*, 2012, **41**(33), 9799–10106.



- 3 (a) I. Lindqvist, *Ark. Kemi*, 1953, **5**, 247; (b) E. J. Graeber and B. Morosin, *Acta Crystallogr., Sect. B: Struct. Crystallogr. Cryst. Chem.*, 1977, **33**, 2137.
- 4 (a) S. Si Larbi, D. Bodirot and B. Spinner, *Rev. Chim. Miner.*, 1976, **13**, 497–507; (b) A. Goiffon and B. Spinner, *Talanta*, 1977, **24**, 130–132.
- 5 M. Nyman, *Dalton Trans.*, 2011, **40**, 8049–8058.
- 6 (a) M. Nyman, F. Bonhomme, T. M. Alam, M. A. Rodriguez, B. R. Cherry, J. L. Krumhansl, T. M. Nenoff and A. M. Sattler, *Science*, 2002, **297**, 996–998; (b) M. Nyman, F. Bonhomme, T. M. Alam, J. B. Parise and G. M. B. Vaughan, *Angew. Chem., Int. Ed.*, 2004, **43**, 2787–2792; (c) T. M. Anderson, S. G. Thoma, F. Bonhomme, M. A. Rodriguez, H. Park, J. B. Parise, T. M. Alam, J. P. Larentzos and M. Nyman, *Cryst. Growth Des.*, 2007, **7**, 719–723; (d) F. Bonhomme, J. P. Larentzos, T. M. Alam, E. J. Maginn and M. Nyman, *Inorg. Chem.*, 2005, **44**, 1774–1785; (e) M. Nyman, A. J. Celestian, J. B. Parise, G. P. Holland and T. M. Alam, *Inorg. Chem.*, 2006, **45**, 1043–1052; (f) M. Nyman, J. P. Larentzos, E. J. Maginn, M. E. Welk, D. Ingersoll, H. Park, J. B. Parise, I. Bull and F. Bonhomme, *Inorg. Chem.*, 2007, **46**, 2067–2079; (g) Y. Hou, M. Nyman and M. Rodriguez, *Angew. Chem., Int. Ed.*, 2011, **50**, 12514–12517.
- 7 (a) M. Nyman, L. J. Criscenti, F. Bonhomme, M. A. Rodriguez and R. T. Cygan, *J. Solid State Chem.*, 2003, **176**, 111–119; (b) C. A. Ohlin, E. M. Villa, J. C. Fettinger and W. H. Casey, *Angew. Chem., Int. Ed.*, 2008, **47**, 5634–5636; (c) C. A. Ohlin, E. M. Villa, J. C. Fettinger and W. H. Casey, *Dalton Trans.*, 2009, 2677–2678; (d) J.-Y. Niu, G. Chen, J.-W. Zhao, P.-T. Ma, S.-Z. Li, J.-P. Wang, M.-X. Li, Y. Bai and B.-S. Ji, *Chem.-Eur. J.*, 2010, **16**, 7082–7086; (e) G. Guo, Y. Xu, J. Cao and C. Hu, *Chem. Commun.*, 2011, **47**, 9411–9413; (f) G. Guo, Y. Xu, J. Cao and C. Hu, *Chem.-Eur. J.*, 2012, **18**, 3493–3497; (g) P. Huang, C. Qin, X.-L. Wang, C.-Y. Sun, G.-S. Yang, K.-Z. Shao, Y.-Q. Jiao, K. Zhou and Z.-M. Su, *Chem. Commun.*, 2012, **48**, 103–105; (h) J.-H. Son, C. A. Ohlin and W. H. Casey, *Dalton Trans.*, 2012, **41**, 12674–12677; (i) J.-H. Son, C. A. Ohlin, E. C. Larson, P. Yu and W. H. Casey, *Eur. J. Inorg. Chem.*, 2013, 1748–1753; (j) J.-H. Son, C. A. Ohlin, R. L. Johnson, P. Yu and W. H. Casey, *Chem.-Eur. J.*, 2013, **19**, 5191–5197; (k) J.-H. Son, C. A. Ohlin and W. H. Casey, *Dalton Trans.*, 2013, **42**, 7529–7533.
- 8 (a) B. W. Dale and M. T. Pope, *Chem. Commun.*, 1967, 792; (b) B. W. Dale, J. M. Buckley and M. T. Pope, *J. Chem. Soc. A*, 1969, 301–304; (c) C. M. Flynn Jr. and G. D. Stucky, *Inorg. Chem.*, 1969, **8**, 332–334; (d) C. M. Flynn Jr. and G. D. Stucky, *Inorg. Chem.*, 1969, **8**, 335–344.
- 9 D. Atencio, J. M. V. Coutinho, A. C. Doriguetto, Y. P. Mascarenhas, J. Ellena and V. C. Ferrari, *Am. Mineral.*, 2008, **93**, 81–87.
- 10 (a) R. D. Peacock and T. J. R. Weakley, *J. Chem. Soc. A*, 1971, 1836–1839; (b) J. Iball, J. N. Low and T. J. R. Weakley, *J. Chem. Soc., Dalton Trans.*, 1974, 2021–2024; (c) T. Ozeki, M. Takahashi and T. Yamase, *Acta Crystallogr., Sect. C: Cryst. Struct. Commun.*, 1992, **48**, 1370–1374; (d) M. Sugeta and T. Yamase, *Bull. Chem. Soc. Jpn.*, 1993, **66**, 444–449.
- 11 A. V. Besserguenev, M. H. Dickman and M. T. Pope, *Inorg. Chem.*, 2001, **40**, 2582–2586.
- 12 J. Fuchs, H. Hartl and W. Schiller, *Angew. Chem., Int. Ed. Engl.*, 1973, **12**, 420.
- 13 (a) C. Tanielian, *Coord. Chem. Rev.*, 1998, 1165–1181; (b) I. N. Lykakis, C. Tanielian, R. Seghrouchni and M. Orfanopoulos, *J. Mol. Catal. A: Chem.*, 2007, **262**, 176–184; (c) M. D. Tzirakis, I. N. Lykakis and M. Orfanopoulos, *Chem. Soc. Rev.*, 2009, **38**, 2609–2621; (d) I. Ryu, A. Tani, T. Fukuyama, D. Ravelli, S. Montanaro and M. Fagnoni, *Org. Lett.*, 2013, **15**, 2554–2557.
- 14 (a) C. M. Flynn Jr. and M. T. Pope, *J. Am. Chem. Soc.*, 1970, **92**, 85–90; (b) S. Liu, D. Li, L. Xie, H. Cheng, X. Zhao and Z. Su, *Inorg. Chem.*, 2006, **45**, 8036–8040.
- 15 (a) D. Honda, S. Ikegami, T. Inoue, T. Ozeki and A. Yagasaki, *Inorg. Chem.*, 2007, **46**, 1464–1470; (b) S. Ikegami, K. Kani, T. Ozeki and A. Yagasaki, *Chem. Commun.*, 2010, **46**, 785–787.

